

## Supporting Information for

### Discovery of BAZ2A Bromodomain Ligands

Dimitrios Spiliotopoulos<sup>1</sup>, Eike-Christian Wamhoff<sup>2,3</sup>, Graziano Lolli<sup>1,4</sup>, Christoph Rademacher<sup>2,3</sup>  
and Amedeo Caflisch<sup>1</sup>

*Author Affiliations:*

<sup>1</sup>Department of Biochemistry, University of Zürich, Winterthurerstrasse 190, CH-8057 Zürich, Switzerland

<sup>2</sup>Department of Biomolecular Systems, Max Planck Institute of Colloids and Interfaces, Am Mühlenberg 1, 14424 Potsdam, Germany

<sup>3</sup>Institute of Chemistry and Biochemistry, Department of Biology, Chemistry, and Pharmacy, Freie Universität Berlin, Takustraße 3, 14195 Berlin, Germany

<sup>4</sup>Protein Crystallography and Structure-Based Drug Design, CIBIO, University of Trento, via Sommarive 9, 38123 Povo (TN), Italy

Correspondence to Graziano Lolli, Christoph Rademacher and Amedeo Caflisch: [graziano.lolli@unitn.it](mailto:graziano.lolli@unitn.it); [christoph.rademacher@mpikg.mpg.de](mailto:christoph.rademacher@mpikg.mpg.de); [caflisch@bioc.uzh.ch](mailto:caflisch@bioc.uzh.ch).

## Table of Contents

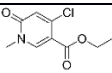
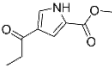
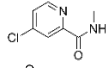
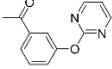
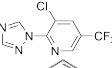
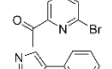
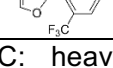
<b>Page</b>	<b>Contents</b>
	<b>Tables:</b>
S3	Table S1: 2D structures and SEED energy terms of the top poses for each of the twenty molecules predicted in silico as BAZ2A bromodomain ligands.
S4	Table S2. Ligand-based NMR spectroscopy validation of the seven molecules predicted in silico as BAZ2A bromodomain ligands.
S5	Table S3. Data collection and refinement statistics.
	<b>Figures:</b>
S6	Figure S1. Distribution of molecular weight, heavy atom count, rotatable bonds, H-bond donors, acceptors, and logP calculated with RDKit for the docked library of 1413 small molecules.
S7	Figure S2. Insights into the energetic terms calculated using SEED for the two top poses of compounds <b>1</b> , <b>2</b> , <b>3</b> , and <b>4</b> .
S8	Figure S3. Competition binding assays for compounds <b>1–4</b> .
S9	Figure S4. Electron density maps define well the binding poses of the small molecules.
S10	Figure S5. Structural overlap reveals significant differences in the binding modes of compounds <b>2</b> and <b>3</b> in BAZ2A and BAZ2B with respect to bromodomain inhibitors with similar head groups reported previously.
S11	Figure S6. Polar interactions between the Asn1823 (BAZ2A, cyan) or Asn1894 (BAZ2B, magenta) backbone amide and bromodomain inhibitors.
S12	Figure S7. Comparison of the <i>holo</i> structures of the BAZ2A bromodomain.
S13	<b>References</b>

**Table S1. 2D structures and contributions to the binding energy (in kcal/mol) for the twenty molecules predicted as BAZ2A bromodomain ligands by the docking program SEED<sup>a</sup>**

	2D structure	intermolecular		electrostatic desolvation		$\Delta G_{\text{elect}}$	total energy
		vdW	elect.	receptor	fragment		
1		-18.5	-7.9	3.4	6.6	2.1	-16.4
2		-18.3	-4.1	2.9	3.5	2.3	-16.0
3		-22.9	-5.1	4.7	5.1	4.7	-18.2
4		-17.9	-3.2	2.4	2.6	1.8	-16.1
5		-18.6	-5.5	2.8	2.4	-0.3	-18.9
6		-17.6	-3.9	2.7	2.4	1.2	-16.4
7		-18.2	-6.0	2.9	3.4	0.3	-17.9
8		-18.7	-8.0	2.4	4.4	-1.2	-19.9
9		-18.9	-6.2	3.1	4.5	1.4	-17.5
10		-19.7	-5.8	2.8	3.8	0.8	-18.9
11		-17.5	-3.2	2.3	3.5	2.6	-14.9
12		-20.0	-3.5	4.5	3.1	4.1	-15.9
13		-17.9	-6.7	3.1	3.9	0.3	-17.6
14		-17.0	-7.9	2.8	7.4	2.3	-14.7
15		-16.5	-6.5	2.8	4.3	0.6	-15.9
16		-21.3	-3.0	2.6	4.9	4.5	-16.8
17		-17.6	-4.8	2.6	3.0	0.7	-16.8
18		-17.2	-4.7	2.6	2.7	0.7	-16.6
19		-16.9	-6.5	2.4	3.0	-1.1	-18.0
20		-23.9	-3.6	4.2	4.9	5.4	-18.5

<sup>a</sup> The SEED total energy (total energy) is calculated as the sum of the intermolecular van der Waals energy (vdW), the intermolecular electrostatics energy calculated in the solvent using a continuum dielectric representation (elect.), the electrostatic desolvation energy of the receptor and ligand upon binding (receptor and fragment, respectively).  $\Delta G_{\text{elect}}$  is the total electrostatic contribution to the binding free energy in the solvent, calculated as the sum of intermolecular electrostatic energy and desolvation penalties.

**Table S2. Ligand-based NMR spectroscopy validation of the seven molecules predicted *in silico* as BAZ2A bromodomain ligands**

2D structure	HAC <sup>a</sup>	NMR screening <sup>b</sup>			BROMOScan % <sup>c</sup>
		<sup>1</sup> H	STD	CPMG	
	14	+	+	+	0.7
	13	+	+	+	8.4
	11	+	+	+	33
	16	+	+	+	27
	16	-	+	+	52
	10	-	+	+	60
	15	+	-	+	63

<sup>a</sup> HAC: heavy atom count. <sup>b</sup> NMR screening techniques included <sup>1</sup>H, saturation transfer difference (STD) NMR and Carr-Purcell-Meiboom-Gill (CPMG). <sup>c</sup> Binding of the BAZ2A bromodomain to an acetylated peptide in the presence of 0.5 mM of the ligand with respect to DMSO solution, with lower percentage values indicating stronger inhibition

**Table S3. Data collection and refinement statistics**

	BAZ2A / 1	BAZ2A / 2	BAZ2A / 3	BAZ2A / 4	BAZ2B / 1	BAZ2B / 2	BAZ2B / 3
<b>Data Collection</b>							
<b>Space group</b>	P3 <sub>1</sub> 21	P3 <sub>1</sub> 21	P3 <sub>1</sub> 21	P3 <sub>1</sub> 21	C222 <sub>1</sub>	C222 <sub>1</sub>	C222 <sub>1</sub>
<b>Unit-cell parameters (Å)</b>	a = 95.74 b = 95.74 c = 32.96	a = 95.24 b = 95.24 c = 32.96	a = 95.55 b = 95.55 c = 32.84	a = 94.86 b = 94.86 c = 32.75	a = 79.95, b = 96.75, c = 57.98	a = 81.12, b = 96.10, c = 57.48	a = 80.70, b = 96.71, c = 57.55
<b>Wavelength (Å)</b>	1.00	1.00	1.00	1.00	1.00	1.00	1.00
<b>Resolution (Å)</b>	47.87-2.10 (2.16-2.10)	47.62-2.30 (2.38-2.30)	27.06-2.65 (2.16-2.10)	27.38-2.80 (2.95-2.80)	48.38-1.95 (2.00-1.95)	42.15-1.90 (1.94-1.90)	42.17-2.10 (2.16-2.10)
<b>R<sub>merge</sub> (%)</b>	20.6 (107.4)	19.1 (113.2)	26.8 (93.6)	31.8 (134.7)	7.7 (78.5)	4.8 (73.2)	7.0 (86.1)
<b>R<sub>meas</sub> (%)</b>	21.8 (113.0)	20.0 (118.6)	28.3 (100.1)	33.5 (143.2)	8.3 (84.2)	5.1 (78.8)	7.6 (93.1)
<b>R<sub>pim</sub> (%)</b>	7.0 (35.1)	6.1 (35.2)	9.0 (34.7)	10.4 (48.0)	3.1 (30.2)	1.9 (29.0)	2.9 (34.7)
<b>&lt;I/σ(I)&gt;</b>	9.2 (2.4)	11.0 (2.4)	7.0 (2.0)	7.1 (2.0)	14.1 (2.2)	23.0 (2.4)	16.6 (2.3)
<b>CC<sup>1/2</sup></b>	0.995 (0.785)	0.996 (0.877)	0.979 (0.741)	0.984 (0.699)	0.999 (0.930)	0.999 (0.912)	0.999 (0.858)
<b>Completeness (%)</b>	100 (100)	100 (99.9)	99.9 (100)	99.5 (100)	99.9 (99.7)	99.9 (99.7)	99.8 (100)
<b>Multiplicity</b>	9.7 (10.1)	10.8 (11.3)	9.6 (8.2)	9.8 (8.7)	7.2 (7.7)	7.2 (7.3)	6.7 (7.1)
<b>Refinement</b>							
<b>Resolution (Å)</b>	31.34-2.10	31.18-2.30	27.06-2.65	27.38-2.80	48.38-1.95	42.15-1.90	37.02-2.10
<b>R<sub>work</sub>/R<sub>free</sub> (%)</b>	19.2/22.2	20.3/23.6	21.3/25.3	21.8/25.2	18.0/21.8	17.7/20.1	18.3/21.9
<b>R.m.s. deviations</b>							
<b>Bond lengths (Å)</b>	0.007	0.002	0.002	0.005	0.006	0.007	0.008
<b>Bond angles (°)</b>	1.0	0.7	0.6	0.9	1.0	1.1	1.0
<b>PDB entry</b>	5MGJ	5MGK	5MGL	5MGM	5MGE	5MGF	5MGG

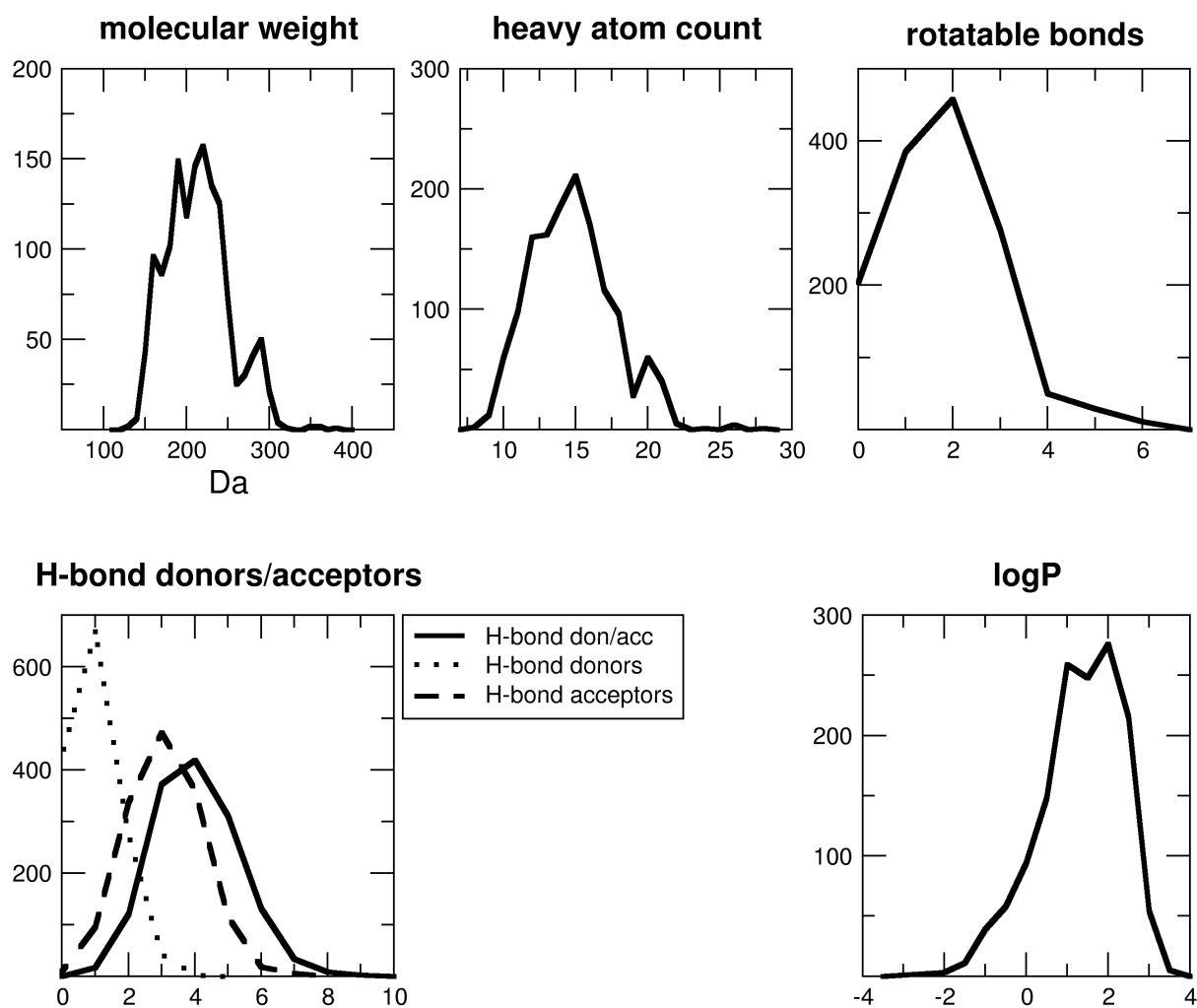


**Figure S1.** Distribution of molecular weight, heavy atom count, rotatable bonds, H-bond donors, acceptors, and logP calculated with RDKit for the docked library of 1413 small molecules.

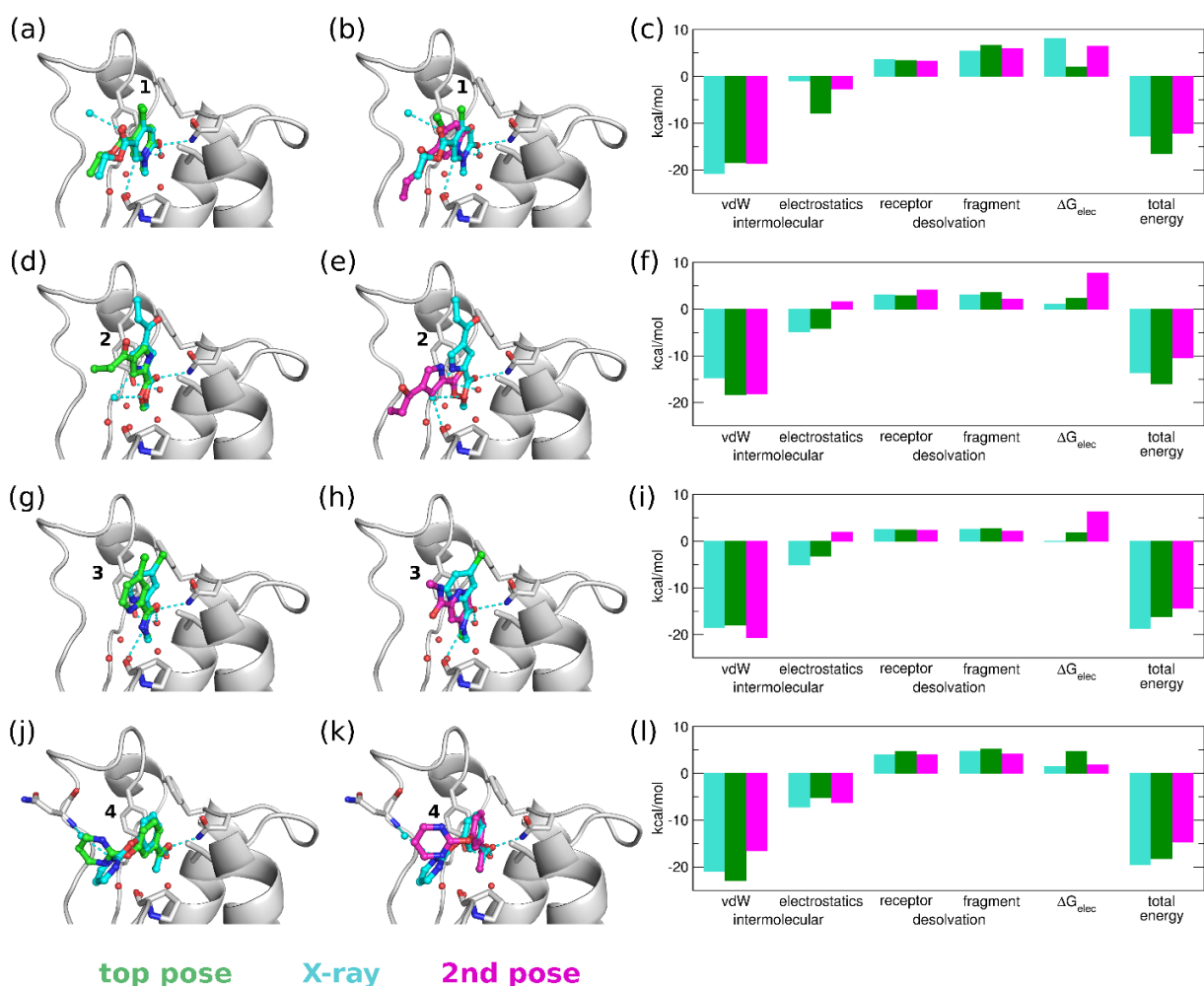


**Figure S2.** Insights into the energetic terms calculated using SEED [1, 2] for the two top poses of compounds 1 (a–c), 2 (d–f), 3 (g–i), and 4 (j–l). The BAZ2A bromodomain is shown as a cartoon and sticks with white carbon atoms, whereas the ligands are shown as sticks. The color coding is consistent in all panels (cyan, green, and magenta for binding mode in the crystal structure, top pose and 2<sup>nd</sup> best pose according to total SEED energy, respectively). (c, f, i, l) The contributions to the binding energy are: the intermolecular van der Waals energy, the intermolecular electrostatic energy calculated in the solvent using a continuum-dielectric representation, the electrostatic desolvation penalties of the receptor and ligand upon binding. These terms sum up to the total energy. The electrostatic contribution to the binding free energy in the solvent ( $\Delta G_{elec}$ ) is the sum of intermolecular electrostatic energy and desolvation penalties.

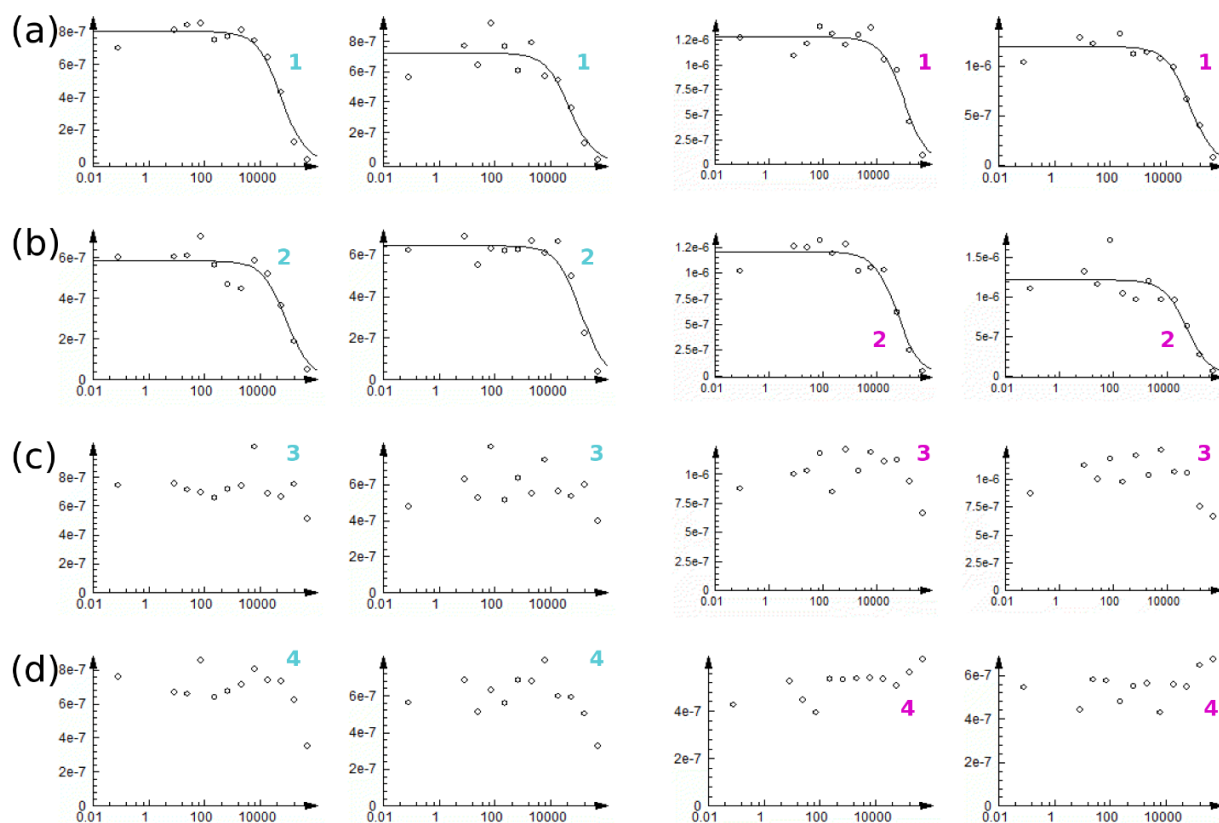


**Figure S3.** Competition binding assays for compounds 1–4. Dose-response curves in duplicates for the compounds 1 (a), 2 (b), 3 (c), and 4 (d) tested for binding to the BAZ2A and BAZ2B bromodomains (cyan and magenta, respectively) in the BROMOscan competition binding assay. Experiments were performed with a final DMSO concentration of 0.09%.



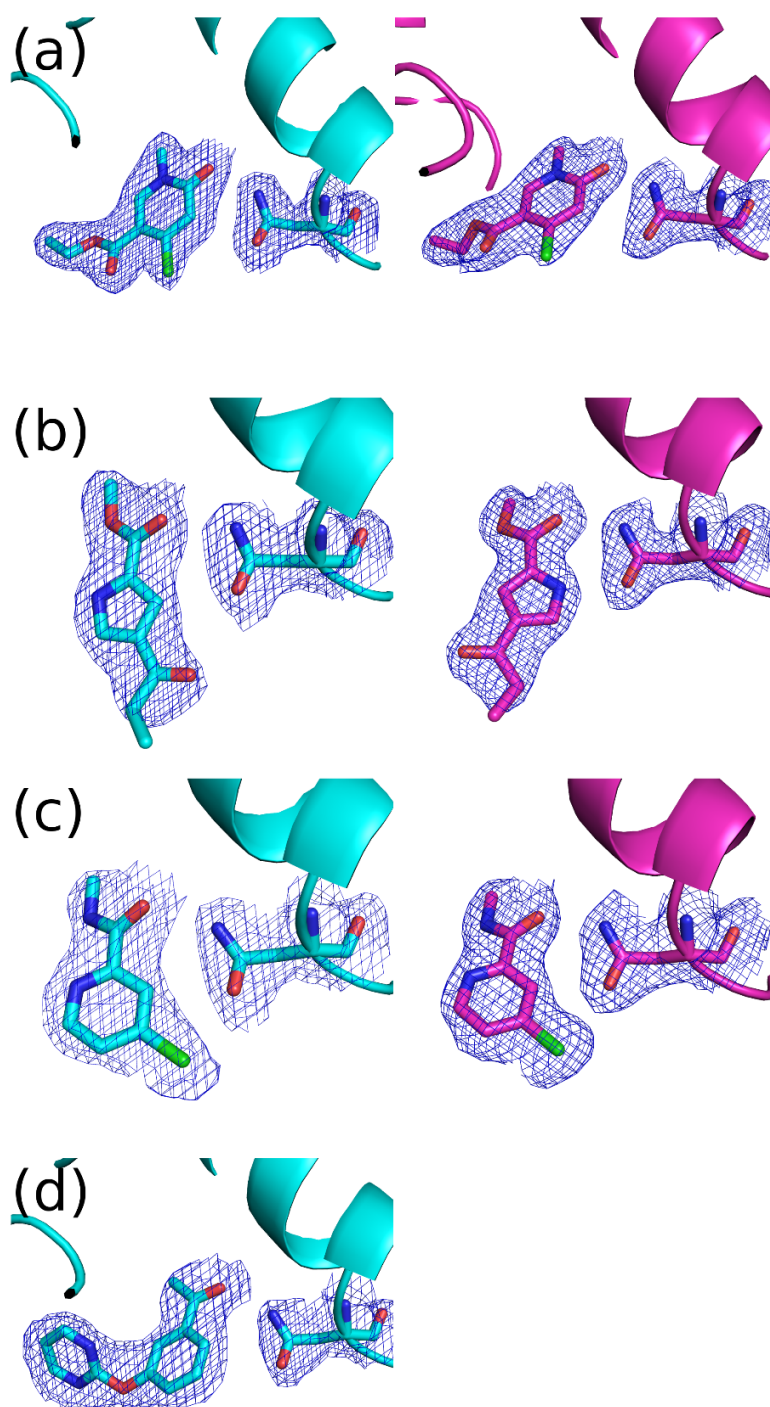


**Figure S4.** Electron density maps define well the binding poses of the small molecules.  $2F_o - F_c$  maps contoured at  $1\sigma$  are shown for compounds and the conserved Asn (1873 in BAZ2A and 1944 in BAZ2B) for the hits **1** (a), **2** (b), **3** (c), and **4** (d). Carbon atoms in the BAZ2A and BAZ2B structures are colored in cyan and magenta, respectively.

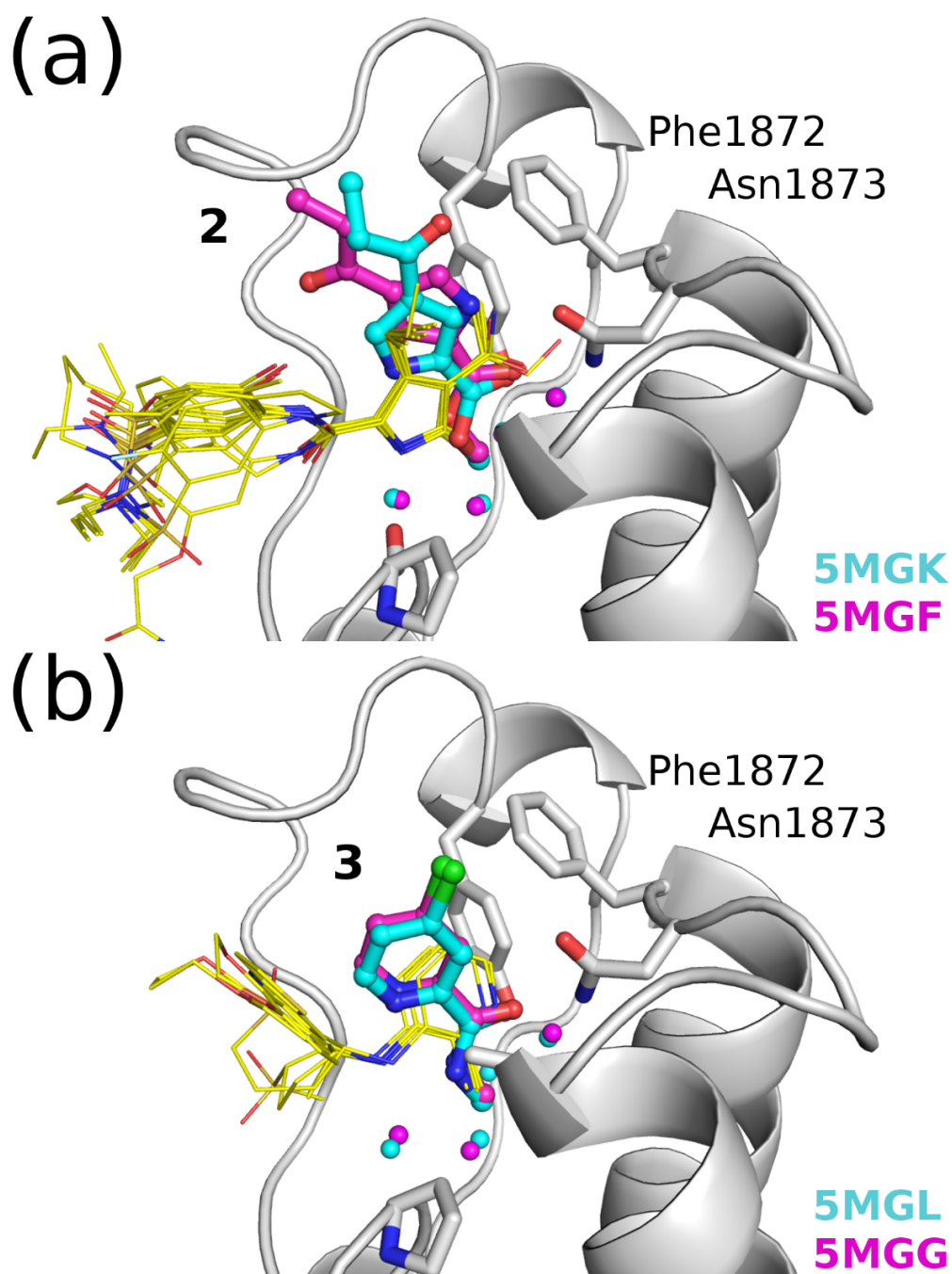


**Figure S5.** Structural overlap reveals significant differences in the binding modes of compounds **2** and **3** in BAZ2A (carbon atoms of ligand and water molecules in cyan) and BAZ2B (magenta) with respect to bromodomain inhibitors with similar head groups reported previously (yellow). The structural overlap is based on the backbone atoms of the bromodomains, and only the BAZ2A structure is shown (gray) to avoid overcrowding. (a) The BAZ2A/B ligand **2** is shown with the tetra-substituted acetylpyrrole inhibitors of the BET bromodomains [3] (yellow). (b) The BAZ2A/B ligand **3** is shown with the 3-amino-2-methylpyridine derivatives presented in [4].

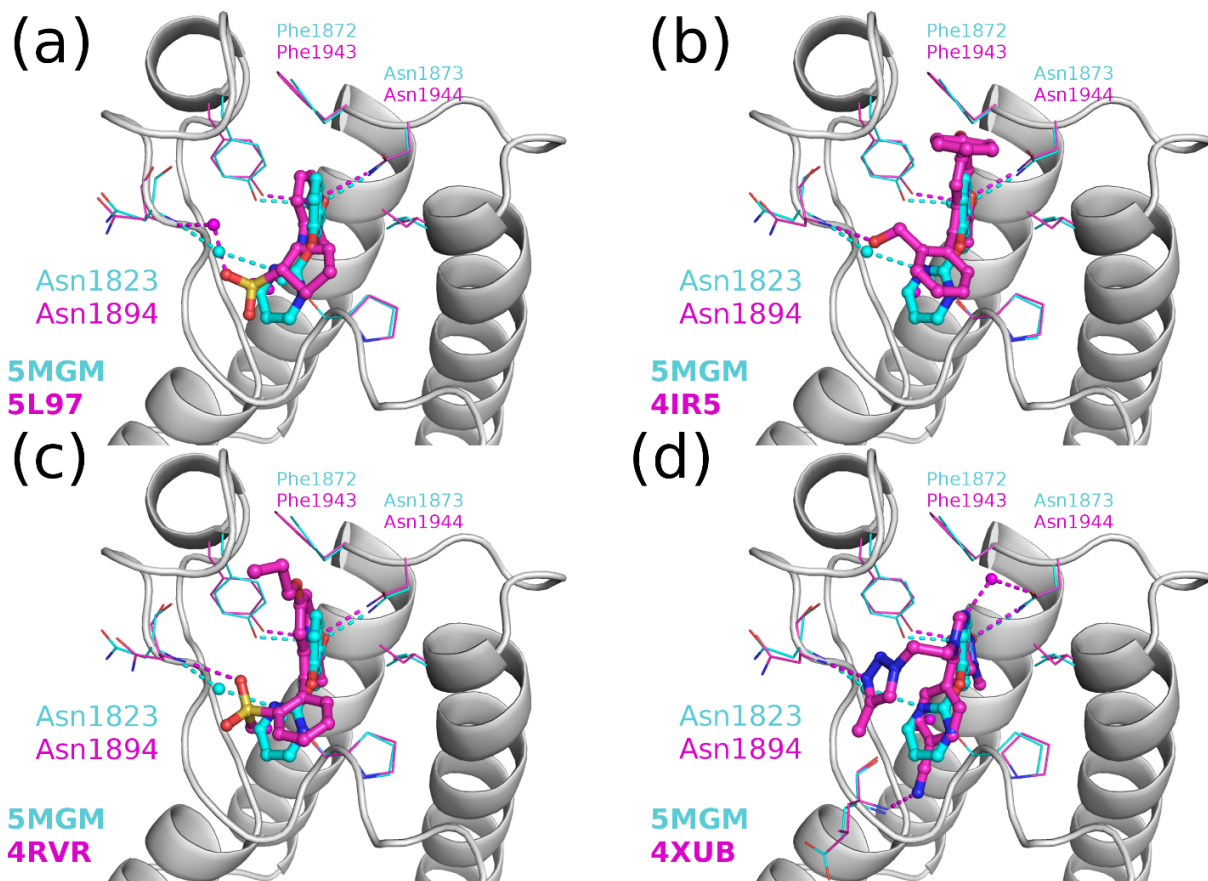


**Figure S6.** Comparison of compound **4** with previously reported ligands and their polar interactions with the Asn1823 (BAZ2A, cyan) or Asn1894 (BAZ2B, magenta) backbone amide. BAZ2B bromodomain-binding small molecules (sticks) that interact with the backbone of Asn1894 include (a) a ligand reported previously by us [4], (b) **24** (GSK2838097A) [5], (c) **21** [5], and (d) **25** (BAZ2-ICR) [6]. Note that the hydrogen bond is water-bridged for compound **4** (cyan, PDB code 5MGM) and for the small molecule in panel A, while it is direct for the remaining inhibitors. Crystallographic water molecules are shown as spheres and polar interactions are highlighted by dashed lines. The carbon atoms, crystallographic water molecules, and polar interactions for the BAZ2A and BAZ2B structures are shown in cyan and magenta, respectively.

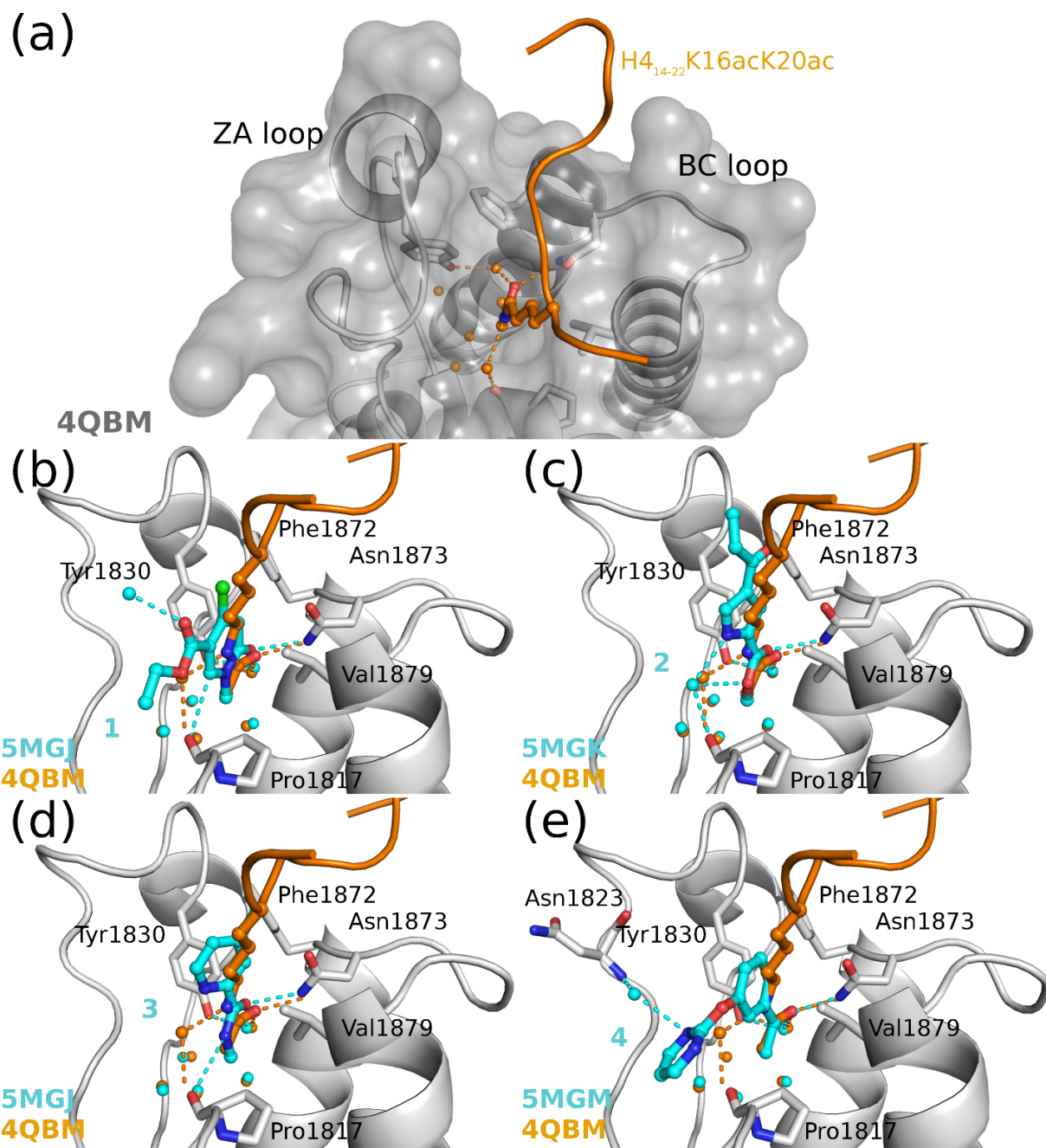


**Figure S7.** Comparison of the *holo* structures of the BAZ2A bromodomain. (a) Structure of the BAZ2A bromodomain (gray) complexed with the diacetylated histone H4 peptide (ochre). (b–e) Comparison of the binding mode of the natural ligand acetyllysine with the fragment hits discovered *in silico* (b) **1**, (c) **2**, (d) **3**, and (e) **4** (carbon atoms in cyan). Crystallographic water molecules and polar contacts are shown with spheres and dashed lines, respectively, using the same color code.

## REFERENCES:

- [1] Majeux N, Scarsi M, Apostolakis J, Ehrhardt C, Caflisch A. Exhaustive Docking of Molecular Fragments With Electrostatic Solvation. *Proteins* 1999;37:88-105.
- [2] Majeux N, Scarsi M, Caflisch A. Efficient electrostatic solvation model for protein-fragment docking. *Proteins* 2001;42:256-68.
- [3] Hügler M, Lucas X, Weitzel G, Ostrovskiy D, Breit B, Gerhardt S, et al. 4-Acyl Pyrrole Derivatives Yield Novel Vectors for Designing Inhibitors of the Acetyl-Lysine Recognition Site of BRD4(1). *J. Med. Chem.* 2016;59:1518-30.
- [4] Marchand JR, Lolli G, Caflisch A. Derivatives of 3-amino-2-methylpyridine as BAZ2B Bromodomain Ligands: in silico Discovery and in crystallo Validation. *J. Med. Chem.* 2016;59:9919-27.
- [5] Chen P, Chaikuad A, Bamborough P, Bantscheff M, Bountra C, Chung CW, et al. Discovery and Characterization of GSK2801, a Selective Chemical Probe for the Bromodomains BAZ2A and BAZ2B. *J. Med. Chem.* 2016;59:1410-24.
- [6] Drouin L, McGrath S, Vidler LR, Chaikuad A, Monteiro O, Tallant C, et al. Structure enabled design of BAZ2-ICR, a chemical probe targeting the bromodomains of BAZ2A and BAZ2B. *J. Med. Chem.* 2015;58:2553-9.